

## Enriching carbonylated proteins inside a microchip through the use of oxalyldihydrazide as a crosslinker†

Bryant C. Hollins,<sup>ab</sup> Steven A. Soper<sup>c</sup> and June Feng<sup>\*ab</sup>

Received 27th January 2012, Accepted 9th March 2012

DOI: 10.1039/c2lc40103g

We report a proof of principle study for the use of oxalyldihydrazide as a crosslinker for enrichment of carbonylated proteins within a microfluidic chip. Surface modification steps are characterized and analyzed using analytical techniques. We use oxidized cytochrome c as our model protein and demonstrate the chip's ability to capture carbonylated targets. After 100 min of continuous loading, the chip is capable of capturing 7.5 μg of carbonylated protein. All the proteins captured are eluted out of the chip using the elution protocol. Finally, we demonstrate the chip's specificity for oxidized targets by mixing oxidized cytochrome c and TRITC-BSA, with cytochrome c in low abundance. The results show that the chip is efficient at finding its target when unoxidized proteins are present. This is the first report to suggest the use of immobilized oxalyldihydrazide on a microchip as an enrichment methodology for low abundance proteins in a sample.

### Introduction

Protein oxidation occurs as a result of exposure to oxidative stress.<sup>1–4</sup> Protein oxidation has been implicated in aging and many age-related disease states.<sup>4–7</sup> Protein oxidation is a post-translational modification (PTM) to proteins and can occur in over 35 different ways.<sup>8</sup> One form of protein oxidation is carbonylation, an irreversible PTM of proteins where an aldehyde bonds to an amino acid residue, most commonly lysine, proline, theorenine or arginine.<sup>7,8</sup> These proteins are used as common markers for oxidative stress within a system.<sup>4,9</sup> Currently, the chemical probes for the analysis of carbonylated proteins include 2,4-dinitrophenylhydrazide (DNPH), biotin-containing probe, *etc.*<sup>10</sup>

Immunoassays are the most common techniques used for detecting carbonylated proteins from samples.<sup>11,12</sup> Carbonylated proteins are primarily detected based upon derivatization of 2,4-dinitrophenylhydrazide (DNPH). The derivatized product is then treated with DNP antibodies labelled with peroxidase secondary antibodies.<sup>13,14</sup> Carbonyls are also detected using a colorimetric assay. DNPH is derivatized with carbonyls and a hydrazone bond is formed. The absorbance of the hydrazone bond is measured to verify its presence<sup>15</sup> and gives quantitative

measurement of carbonyls. A limitation of this technique is the high quantities of proteins needed for this colorimetric assay.<sup>15</sup>

In proteomic studies, these proteins often require enrichment due to their low abundance. One technique for enrichment is the use of biotin tagging and avidin affinity chromatography.<sup>2,16</sup> Commonly, low abundance proteins are derivatized with biotin hydrazide and captured on an immobilized avidin column. The biotinylated proteins are eluted through the use of high biotin salt. The labelled proteins can be further analyzed using standard proteomic techniques.<sup>2,17–19</sup> One limitation of this technique lies in the elution step because high volumes of biotin are needed to replace the proteins on the column. Thus, the already minuscule amount of proteins are further diluted in the elution and additional pre-concentration steps, such as using a spin column to remove excess solution, are required before the mass spectrometry analysis. Additionally, this sample preparation method requires biotin derivatization followed by removal of excess biotin hydrazide before performing biotin-avidin affinity chromatography. These steps could take from several hours to overnight.<sup>2,5</sup> Alternatively, monomeric avidin or streptavidin beads have been reported for affinity based capture after linking carbonylated proteins with biotin hydrazide.<sup>16</sup>

Another enrichment method is facilitated using surface modified magnetic or nonmagnetic beads for immunoprecipitation. In general, after derivatization, carbonylated proteins forms a covalent bond with DNPH and the formed DNP-tagged proteins were immunoprecipitated by Protein A or G beads tethered with anti-DNP antibodies.<sup>20,21</sup>

The use of microelectromechanical systems (MEMS) provides a promising platform for protein analysis,<sup>12</sup> especially for low abundant proteins where samples may be limited or difficult to obtain. Microfluidic chips are composed of materials such as

<sup>a</sup>Department of Biomedical Engineering, Louisiana Tech University, Biomedical Engineering Center 211, Ruston, LA, USA.

E-mail: junefeng@latech.edu; Fax: 318-257-4000; Tel: 318-257-5236

<sup>b</sup>Institute of Micromanufacturing, Louisiana Tech University, Ruston, LA, USA

<sup>c</sup>Department of Chemistry, Louisiana State University, Choppin Hall 212 Baton Rouge, LA, USA

† Electronic supplementary information (ESI) available: Figures S1–S4. See DOI: 10.1039/c2lc40103g/

glass or silicon and are usually simple to construct using basic photolithography techniques. Recently, polymeric chips have become increasingly popular due to their versatility and lower cost.<sup>22,23</sup> Particularly, using high precision micromilling for metal mold master fabrication is desirable for researchers who do not have access to extensive lithography based equipment. The low cost and mass production allow for these chips to be disposable, reducing the likelihood of cross-contamination between samples on a reused chip. The advantages, such as fast analysis, high throughput, and low reagent consumption, offered by BioMEMS compared to conventional techniques make BioMEMS a great choice for low abundance samples.

We present in this report a microfluidic device that can selectively capture carbonylated proteins from a sample. *In vitro* oxidized cytochrome c is used as a model protein. Capture is achieved through specific manipulation of the polymethyl (methacrylate) (PMMA) polymer to attach oxalyldihydrazide, a crosslinker specific to carbonyls, to the surface of the microchip. We use *in vitro* oxidized BSA to verify the working of the surface modification and *in vitro* oxidized cytochrome c as our target molecule to demonstrate the selectivity of the chip. Finally, we close our study with analysis of the device's ability to capture low abundance target proteins from a mixture containing an excess of a large blocking protein. Surface modification of PMMA is verified through differing analytical techniques. Surface elemental analysis and roughness were examined by X-ray Photoelectron spectroscopy (XPS) and atomic force spectroscopy (AFM), respectively. Additionally, fluorescence microscopy was utilized for chemical functional groups mapping to verify the presence of desired crosslinkers. This work is the first to propose the use of oxalyldihydrazide as a method of carbonylated protein enrichment. By using a crosslinker that is specific to carbonyls, the need for derivatization and extensive washing and preconcentration step afterwards are eliminated. Additionally, to our knowledge, this is the first report of carbonylated protein enrichment through coupling the use of a crosslinker to a microchip.

## Materials and methods

### Materials

Polymethyl-methacrylate (PMMA) sheets were purchased from Goodfellow. 2,4-Dinitrophenylhydrazine (DNPH), EDTA, HEPES, potassium chloride, magnesium chloride, sodium ascorbate, iron(III) chloride, hydrochloric acid, formic acid, *N*-(3-dimethylaminopropyl)-*N'*-ethylcarbodiimide (EDC), albumin, tetramethylrhodamineisothiocyanate (TRITC-BSA) and bovine serum albumin were purchased from Sigma Aldrich (St. Louis, MO). Oxalyldihydrazide was purchased from Alfa Aesar (Ward Hill, MA). *N*-hydroxysuccinimide (NHS) was purchased from Thermo Scientific (Rockford, IL). Naphthalene-2,3-dicarboxaldehyde (NDA) was purchased from Invitrogen (Eugene, OR). Cytochrome c was purchased from EMD Chemicals (Gibbstown, NJ).

### Metal catalyzed oxidation

Bovine serum albumin (BSA) and cytochrome c were dissolved at 10 mg mL<sup>-1</sup> and 5 mg mL<sup>-1</sup>, respectively, in oxidation buffer

(50 mM HEPES buffer, pH 7.4, containing 100 mM KCl and 10 mM MgCl<sub>2</sub>). The proteins were oxidized *in vitro* using metal catalyzed oxidation.<sup>24</sup> Briefly, 30 mL of oxidation buffer containing proteins was supplemented with neutral ascorbic acid and FeCl<sub>3</sub>, to final concentrations of 25 mM and 100 μM, respectively. The mixture was incubated overnight at 37 °C in a shaking bath. Oxidation was terminated by adding EDTA to a final concentration of 1 mM. Proteins were aliquoted and frozen at -20 °C until use. Proteins were diluted to required concentrations prior to experiments. Successful oxidation was confirmed using the spectrophotometric DNPH assay.

### Off-chip protein labelling

Prior to experiments inside the channel, oxidized cytochrome c was labelled with naphthalene-2,3-dicarboxaldehyde (NDA), a fluorogenic probe.<sup>25</sup> Briefly, NDA was dissolved in 100% methanol. 100 μL of 2 mg mL<sup>-1</sup> oxidized cytochrome c was placed in a tube. 400 μL of 10 mM borate buffer (pH 9.4) was added to the tube, followed by 100 μL of 10 mM KCN dissolved in water. Lastly, 400 μL of 5 mM NDA/methanol stock was added to the tube. The tube was allowed to incubate for 30 min at room temperature. Following incubation, the sample was rinsed in an Amicon Ultra-4 centrifugal filter unit (3000 MW cutoff) to remove any unbound NDA. The rinse was done in 10 mM borate buffer for 20 min. The solution was spun down to about 200 μL, and the sample was supplemented with 800 μL of borate buffer to give a total volume of 1 mL.

### Microchip fabrication

The microchip used in these experiments is shown in Fig. 1. The bed of the PMMA channel has microposts of 100 μm diameter. The depth of the channel is 50 μm, and the length of the channel is 12.5 mm. The capture bed is 1 mm wide, containing 150 microposts. The post-to-post spacing is 150 μm. The surface area available for protein capture is 27.4 mm<sup>2</sup>. Because of the width of the channel, the posts are included to prevent the coverslip from collapsing into the channel during annealing.

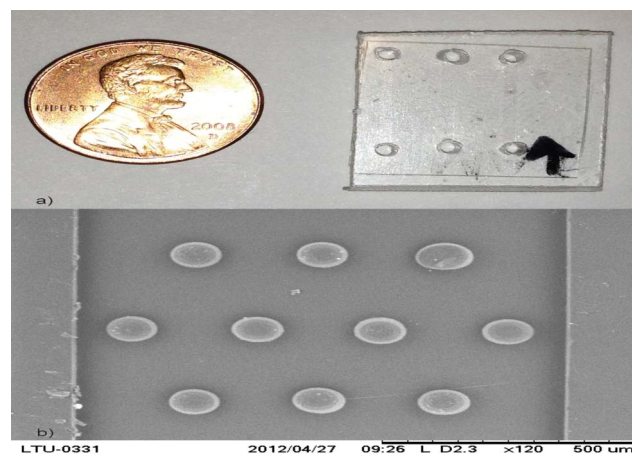


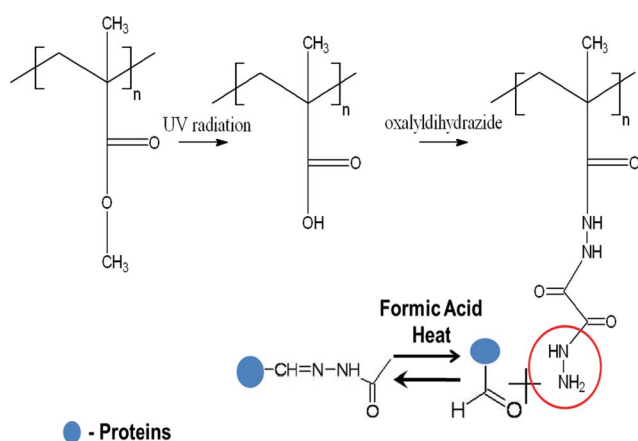
**Fig. 1** SEM image of the microchip showing the internal microposts within the capture bed. The microposts have a diameter of 100 μm. The channel's benchtop size is demonstrated next to a penny. The channel length is 12.5 mm, width 1 mm, and depth 50 μm. Scale bar = 500 μm.

The reservoirs are 1.6 mm in diameter. The chip fabrication process started with micromilling of the mold master. Specifically, the abovementioned microstructures were milled on the surface of a 6.3 mm thick brass plate (alloy 353 engravers brass, McMaster Carr, Atlanta, GA) using a high-precision micromilling machine (Kern Mmp 2522, Kern Micro-und Feinwerktechnik GmbH & Co. KG; Germany). A typical milling cycle started with a rough milling to prepare an approximate shape for subsequent finishing cut. The feed rates were  $20 \text{ mm min}^{-1}$  for a  $50 \mu\text{m}$  drill bit.<sup>26</sup>

PMMA sheets (Plexiglas MC, GE Polymershapes, New Orleans, LA) were cut into 65 mm diameter discs and cleaned by rinsing with 2-propanol and distilled water. After removing residual moisture by placing them in an oven at  $75 \text{ }^\circ\text{C}$  overnight, the milled microstructures were pressed into the chips using a commercial hydraulic press (PHI Precision Press model TS-21-H-C, City of Industry, CA). A home-built vacuum chamber was installed into the hot embossing press to keep ultra low air pressure ( $< 10 \text{ kPa}$ ) for complete filling of the mold master. The embossing was performed at a force of  $5 \text{ kN}$  for  $5 \text{ min}$  at  $155 \text{ }^\circ\text{C}$ . After embossing, injection and collection reservoirs were created by using a drill press and a  $1/16''$  black oxide drill bit. For the final assembly, a thin PMMA cover plate of  $250 \mu\text{m}$  thickness (Goodfellow, Oakdale, PA) was thermo-bonded to the face of micropost array chip. For this purpose, the microfluidic chip and the cover plates were clamped between two  $3'' \times 3''$  glass plates (McMaster) and placed inside a convection oven at  $104 \text{ }^\circ\text{C}$  for  $30 \text{ min}$ . PEEK tubing ( $800 \mu\text{m}$  diameter) was attached to enclosed microchips using EPOXY. Chips were stored until ready for use for experiments.

### PMMA surface modification

PMMA surface modification was accomplished according to Scheme 1. It elucidates the preparation and the use of PMMA chip containing crosslinker with hydrazide functions for the immobilization of carbonylated proteins specifically through the carbonyl and ketone moieties. Generally, three major steps were involved in the modification process: the functionalized PMMA chips were prepared by introducing carboxylic acid groups after



**Scheme 1** The surface modification procedure used on the PMMA. The exposed hydrazide functional group will react with the carbonyls on the target proteins. Following immobilization of the proteins on the hydrazide-modified surface, the hydrazone bond can be reversed using formic acid and heat.

UV radiation, followed by reaction with the crosslinker, oxalylhydrazide. Carbonylated BSA was then reacted with the hydrazide-derivatized microchip to produce stable hydrazone linkages.

Prior to surface modification, the microchips were cleaned using Micro-90 in water and rinsed with 10% isopropanol and water. Chips were dried under a flowing stream of nitrogen and dried in an oven at  $70 \text{ }^\circ\text{C}$  to evaporate any water trapped in the microstructures.  $250 \mu\text{m}$  PMMA cover slips were cut to enclose the microstructures. Both the microchips and cover slips were then exposed to ultraviolet light ( $254 \text{ nm}$ ,  $15 \text{ mW cm}^{-2}$ ) for one hour. After UV exposure, the chips and cover slips were pressed together for annealing. Afterwards, PEEK tubing was attached to the injection and collection reservoirs of the chips. Using a syringe pump,  $100 \mu\text{L}$  of MES buffer containing  $200 \text{ mM}$  EDC and  $50 \text{ mM}$  NHS was flushed through the channel at a flow rate of  $10 \mu\text{L min}^{-1}$  and allowed to incubate for  $30 \text{ min}$ . After the incubation was completed,  $100 \mu\text{L}$  of  $50 \text{ mM}$  oxalylhydrazide dissolved in MES buffer was flushed through the channel at a flow rate of  $10 \mu\text{L min}^{-1}$  and allowed to incubate overnight. The channels were loaded with proteins the following morning. Solutions of NHS, EDC, and oxalylhydrazide were prepared fresh daily. For experiments conducted on PMMA sheets, the same procedure was used for surface modification.

### Validation of surface chemistry

Surface modification was validated at each step of the procedure using a PMMA sheet. Successful UV exposure was demonstrated using water contact angle measurements. All modification steps were analyzed using X-ray Photoelectron Spectroscopy (XPS) and Atomic Force Spectroscopy (AFM). For XPS and AFM studies, PMMA sheets were treated with UV radiation, and then incubated in  $1 \text{ mL}$  of EDC/NHS, oxalylhydrazide and proteins. After each sheet finished its incubation step, it was rinsed in  $\text{dH}_2\text{O}$  and dried under a flowing stream of nitrogen and stored until analysis.

For XPS analysis, all modified and pristine PMMA surfaces were measured by a Karatos AXIS ultra X-ray photoelectron spectrometer using a monochromatic  $\text{Al-K}\alpha$  X-ray source ( $240 \text{ W}$ ) and charge neutralization. The sample analyses were performed with a  $90^\circ$  takeoff angle and spectral peaks were analyzed using the Kratos software.

AFM studies were performed with a commercial instrument (Nanosurf easyScan 2 equipped with a TFT-LCD display). It was operated by silicon SPM-sensor (NanoWorld, Neuchâtel, Switzerland) in contact mode with  $0.2 \text{ N m}^{-1}$  spring constant and  $13 \text{ kHz}$  response frequency. The ammonium-coated detector is of  $2 \mu\text{m}$  thick,  $450 \mu\text{m}$  long and  $50 \mu\text{m}$  wide. All images were recorded in air at room temperature, at a scan speed of  $1.4 \text{ Hz}$ . The background slope was resolved using the program provided by the manufacture. No further filtering was performed.

Oxalylhydrazide immobilization within the chip was demonstrated using a fluorescent analogue, Alexa 488 hydrazide. Alexa 488 hydrazide was loaded as described above, and fluorescence was detected using an Olympus IX-51 Fluorescence Microscope with an attached CCD camera. Images were taken using a  $10\times$  objective and  $500 \text{ ms}$  exposure time. Filter settings for FITC was used for image capture.

## Protein capture

Prior to loading our target protein to the channel, the channel was blocked by loading 75  $\mu\text{L}$  of 2  $\text{mg mL}^{-1}$  BSA at a rate of 5  $\mu\text{L min}^{-1}$ . The BSA solution remained in the channel for 1 h and was then pushed out using air. Following the blocking, 0.2  $\text{mg mL}^{-1}$  of NDA-labeled oxidized cytochrome c was loaded into the channel for 100 min at a rate of 5  $\mu\text{L min}^{-1}$  using a syringe pump. Solution was collected at the collection reservoir every minute for analysis. After loading was completed, the chip was incubated in the dark for two hours. Protein capture was visualized using fluorescence microscopy. For the selective capture study, cytochrome c and TRITC-BSA were mixed, with concentrations of 0.2  $\text{mg mL}^{-1}$  and 0.8  $\text{mg mL}^{-1}$ , respectively, in the same solution and pushed through the channel at 5  $\mu\text{L min}^{-1}$  following BSA blocking. Solution was collected as described above and analyzed every minute.

## Protein elution

Proteins were eluted using 10% formic acid. The channel was filled with formic acid. Formic acid loading was done at a rate of 10  $\mu\text{L min}^{-1}$ . The channel was incubated in an oven at 60  $^{\circ}\text{C}$  for thirty minutes. Borate buffer was also heated to 60  $^{\circ}\text{C}$ . After incubation, the channel was rinsed with borate buffer at a rate of 5  $\mu\text{L min}^{-1}$  to collect the proteins. The rinsing occurred on a hot plate held at a constant 60  $^{\circ}\text{C}$ . The eluted solution was analyzed every minute.

## Results and discussion

### Water contact angle measurement

The surface chemistry was verified using numerous techniques. First, UV modification was confirmed using water contact angle. Carboxyl groups on the surface of PMMA make the surface more hydrophilic. After exposing a PMMA sheet to UV treatment for twenty minutes, a contact angle of  $46.0 \pm 5.7^{\circ}$  ( $n = 3$ ) vs. a contact angle of  $72.2 \pm 7.8^{\circ}$  for pristine, unmodified PMMA. The decrease was not as low as reported values in the literature of  $30^{\circ}$  for a similar exposure time,<sup>27</sup> so UV exposure time was increased to one hour for subsequent experiments. The literature results demonstrate a plateau at around 40 min, so a one hour exposure time was decided upon to generate the expected results.<sup>27</sup> We chose one hour exposure time to compensate for any differences between the setups of the two UV systems used in our studies and the ones used in the literature study. The difference in the system setup could account for the difference between surface contact angles after 20 min.

### Fluorescence microscopy

To ensure that oxalyldihydrazide would bind to the modified PMMA, a fluorescent analogue, Alexa 488 hydrazide, was used in the chip. The rationale for using this analogue was based on the fact that it has the same functional group as the chosen crosslinker. Alexa 488 hydrazide was loaded into the closed microchip in the same fashion as described for the oxalyldihydrazide (detailed in the Experimental section). The fluorescence observed in the channel after a buffer rinse indicated that Alexa 488 hydrazide was immobilized on the surface of the

microchannel. As a control, Alexa 488 hydrazide was incubated in a similar fashion inside a pristine PMMA microchip. After a buffer rinse, no fluorescence was observed within the microchannel from the unmodified PMMA (see Figure S1, ESI†).

### XPS analysis

XPS studies were conducted on PMMA sheets to verify the chemistry used in the surface modification procedure. The samples were prepared modularly, so each new modification built upon the last, as indicated in Scheme 1. The results of the XPS study are shown in Table 1. After UV modification the oxygen content increases, demonstrating the addition of oxygen molecules in the carboxylic acid. The value obtained in this step ( $\text{O}\% = 26.74$ ) matches reported values in the literature ( $\text{O}\% = 26.28$ ) after one hour UV exposure time.<sup>27</sup> After oxalyldihydrazide incubation, an increase in nitrogen is observed, corresponding to the attachment of the hydrazide functionalities is observed. Oxidized BSA was used to demonstrate protein immobilization on the modified surface of PMMA. Protein incubation shows a great increase in nitrogen composition. Because the coverslip was rinsed prior to completing the next step, we attribute the nitrogen increase seen here to BSA immobilization. BSA is a large protein containing numerous nitrogen atoms in its lysine side chains and through its peptide bonds, so the increase in nitrogen content is not surprising. The presence of nitrogen after UV exposure can be contributed to nitrogen present in the air leaking into the sample container. Native BSA was used as well to investigate the results of non-specific binding on the coverslip.

### AFM analysis

PMMA sheets were prepared as indicated in the Experimental section. AFM studies were done to calculate the surface roughness of PMMA following each step of the process. As additional molecules are being placed on the surface of PMMA, the roughness should increase. The results are shown in Table 2. Small roughness increases are observed following UV treatment and oxalyldihydrazide immobilization. These results are expected since the molecules placed on the surface are small. A great increase is observed following oxidized BSA incubation. Because of the size of BSA (66 kDa), a large increase such as this could be expected. A similar increase was observed with native BSA, though not as large.

These experiments were conducted on the PMMA sheets, which were used as received from Goodfellow. Within the microchip, it is important to consider the effect that the micromilling process will have on the surface roughness of the microfluidic channel. Any milling marks present on the mold

**Table 1** Compositional change following each surface modification determined by X-ray photoelectron spectroscopy

Sample	C(at%)	O(at%)	N(at%)	C/O
Native PMMA	78.78	21.22	0	3.71
UV-modified PMMA	70.52	26.74	2.74	2.64
Oxalyldihydrazide Crosslinked PMMA	71.8	18.94	4.24	3.79
Oxidized-BSA-immobilized PMMA	69.97	19.93	10.11	3.51
Native-BSA-immobilized PMMA	70.5	17.72	11.78	3.98

**Table 2** Area surface roughness changes following each surface modification determined by atomic force microscopy

Stage	Area Surface Roughness (RMS)
Native PMMA	4.03 nm
UV-treated PMMA	6.41 nm
Oxalylhydrazide-crosslinked PMMA	9.87 nm
Oxidized BSA-immobilized PMMA	31.5 nm
Native BSA (control)	20.5 nm

master will be transferred to the microfluidic chip, since hot-embossing is a technique capable of replicating structures to the nanometer range.<sup>26</sup> Over time, the characteristics of the mold master can change, resulting in inconsistencies in microstructures. To minimize this problem, a two-fold strategy was employed. First, because of its excellent machining characteristics, brass was used as the mold master. Secondly, the mold master milling was completed using two steps, removal of the bulk material using a large diameter (500  $\mu\text{m}$ ) bit, followed by use of a smaller milling bit for the finer structures of the design.

### Protein capture

NDA-labelled oxidized cytochrome c ( $0.2 \text{ mg mL}^{-1}$ ) was loaded into the channel and allowed to incubate for two hours. During the loading process, the solution that flowed through the channel was collected for spectrophotometric analysis. NDA is a fluorogenic molecule that is only fluorescent after it has reacted with a primary amine group. Because we use BSA as a blocking protein for the channel, it is necessary to remove any unbound NDA prior to loading it into the channel. This removal prevented any blocking BSA from being labelled with the NDA and altering the results obtained. The amount of oxidized cytochrome c captured in the microchip could be quantified using a Nanodrop 3300 spectrophotometer. Fig. 2a shows the protein amounts collected each minute. The total protein mass captured during the continuous injection period of 100 min is  $7.5 \mu\text{g}$ . The plateau seen in Fig. 2a suggest binding of the target molecule to the reactive sites on the surface of the microchannel, allowing for less binding to occur as more proteins are exposed to the chip, indicating a move toward saturation. Chip saturation occurs when all the available reactive sites for binding are consumed on the surface of the modified PMMA.

### Protein elution

Proteins were eluted using formic acid. Formic acid has been demonstrated to break hydrazone bonds when incubated at an elevated temperature.<sup>28</sup> After thirty minutes of incubation at  $60 \text{ }^\circ\text{C}$ , the channel was rinsed with borate buffer. Since the proteins were labelled and injected into the channel using borate buffer, this same medium was chosen to collect the proteins during elution. The solution was collected from the microchip and analyzed using the Nanodrop. We found that all the proteins injected into the channel were eluted within three minutes of continuous injection of borate buffer. The results are shown in Fig. 2b. The total amount of protein eluted was  $8.5 \mu\text{g}$ , resulting in a cumulative elution efficiency of 113%. The cumulative elution efficiency is calculated by measuring the percentage of proteins eluted from the channel and dividing it by the total

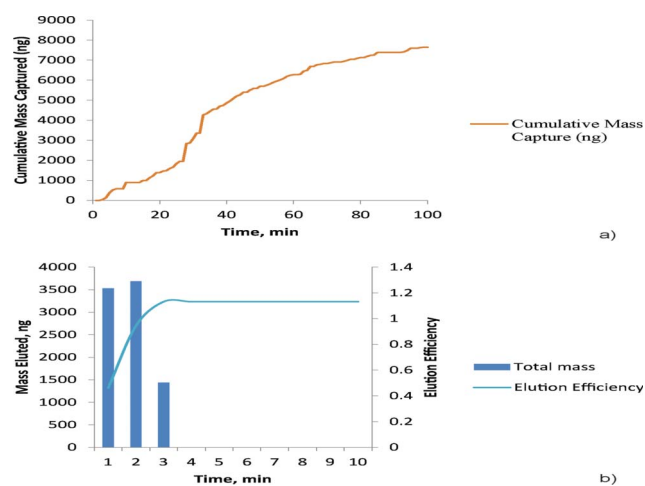


**Fig. 2** The capture and elution efficiency of oxidized cytochrome c in the chip as determined through fluorescence measurement. (a) The capture profile indicates that the chip is approaching saturation. (b) The elution data after ten minutes shows that all the captured proteins are eluted within three minutes.

amount available for elution. Using Fig. 3 as an example, after 1 min  $3.5 \mu\text{g}$  of the  $7.5 \mu\text{g}$  captured are eluted, resulting in a cumulative elution efficiency of 46%. For each additional minute, the total of all the proteins eluted are summed together and divided by the total protein amount available. The elution of the proteins resulted in an increase in the concentration of proteins available from the original stock solution ( $0.2 \text{ mg mL}^{-1}$ ). The new concentration, using the  $15 \mu\text{L}$  required to elute all the proteins, is  $0.53 \text{ mg mL}^{-1}$ , or an increase of 265%.

The additional proteins found in the elution could be a result of additional proteins still inside the injection tubing when injection finished. Because the proteins are allowed to incubate for two hours following injection, any proteins still in the tubing could diffuse into the chip and react with any available surface.

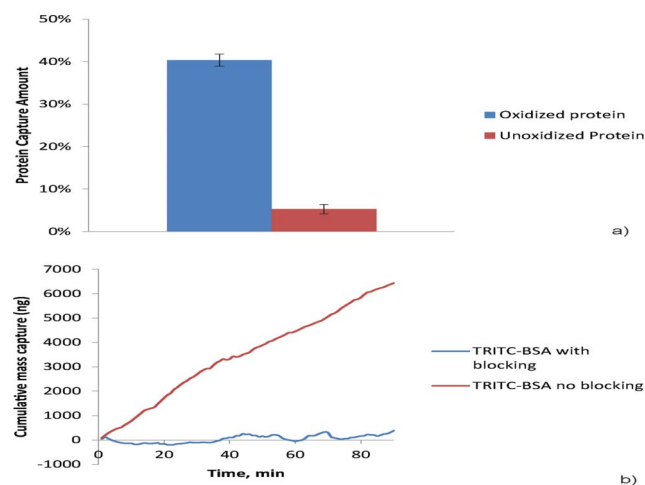


**Fig. 3** (a) The capture percentage of oxidized and unoxidized proteins when injected into the channel as a mixture. The results demonstrate that the chip is highly specific toward oxidized proteins, even when the oxidized protein is in low abundance. (b) The requirement for blocking for the successful discrimination of oxidized and unoxidized proteins within the modified microchip.

We propose that this action occurred, resulting in the additional 1  $\mu\text{g}$  of protein in the elution.

### Protein mixture results

To determine the specificity of the chip for oxidized proteins, oxidized cytochrome *c* labelled with NDA was mixed in low abundance (1 : 4) with TRITC-BSA and injected into the chip. The results of this study are shown in Fig. 3a. The chip was able to capture 40% of the oxidized proteins over the 100 min injection period, whereas only 5% of the unoxidized protein was captured. These results show that, even in low abundance, the chip is highly specific to oxidized proteins. The 5% capture observed from the unoxidized protein (TRITC) could have been the result of some proteins displacing BSA, which was used to block the chip. The results found for the non-specific binding was confirmed by loading TRITC-BSA into a modified channel. These results are shown in Fig. 3b. We found that without blocking, TRITC-BSA is captured within the chip, but after blocking, the capture is significantly lower. These results not only confirm that our reasoning for believing that TRITC-BSA is displacing BSA within the channel is sound, it also speaks to the necessity of blocking the chip prior to enrichment studies in order to increase the chip's discrimination of oxidized and unoxidized proteins.

The effect of fluid dynamics on the ability of the microchip to capture targets is an area of future work. Flow rate studies can be used as a variable for optimizing our capture efficiency. While a faster flow rate would expose the modified surface to additional proteins during the loading process, the effects of shear stress on the crosslinker, oxalyldihydrazide, would have to be considered. To date, no studies have been done on the strength of the bond formed between oxalyldihydrazide and the carboxyl-labelled PMMA surface or the hydrazone bond formed with the carbonyl of the protein. Increasing the flow rate too much could result in breaking the links that provide the ability to capture the target molecules, but a rate too slow will increase the time of the experiment. Therefore, flow rate is one area of optimization necessary in future work. Another area of consideration is the interior geometry of the chip. In this experiment, we used a low-density micropost interior. For future studies, the density of the microposts can be altered to determine if capture efficiency has a dependency on the interior geometry.

The method presented in this article has several advantages over the conventional avidin chromatography technique for carbonylated protein enrichment. One, there is no need to derivatize samples prior to enrichment for our technique. Even though we derivatize our sample with fluorogenic agents, it is not necessary if the device is being used as a preconcentrator. Chromatography requires the sample to be derivatized with biotin, a process that is very time-consuming, including 12 h for dialysis to remove unbound hydrazide. The technique presented in this article takes 4.5 h from protein loading to elution. Also, in order to be effective, avidin chromatography needs at least 2.5 mg of protein, whereas our technique can enrich any amount of protein. As we use a microfluidic chip for enrichment, the amount of sample waste is greatly reduced, and we can collect our proteins in a very small volume, in essence greatly increasing the concentration of low abundance targets. Chromatography

requires a high volume of elution solution, diluting even further an already very dilute sample. Also, when the targets are released from the microchip, they are readily available for future studies with the carbonyl available for additional labelling if necessary. Should the carbonyl need to be relabelled after chromatography, the hydrazone bond between biotin and the carbonyl would require breaking.

For this experiment, oxalyldihydrazide was chosen as the crosslinker. This chemical was chosen because of its small length and lack of a spacer arm. It has been demonstrated that removal of a spacer arm in solid-cation exchange experiments increased protein retention.<sup>29</sup> The authors proposed that the reduction of the spacer arm length provided for enhanced binding opportunity between the adsorbent and the protein.<sup>29</sup> However, in another study, it was demonstrated that the presence of methylene groups in a crosslinker can enhance protein adsorption in affinity chromatography, and that an optimal number of methylene groups in the spacer arm exist for maximum capture.<sup>30</sup> The controversies observed in these studies imply an additional future direction for this work.

An important feature of this process is its versatility. While in this work oxalyldihydrazide was featured for carbonylated protein enrichment, other crosslinkers can be used for other post-translational modifications. One example is the bifunctional crosslinker SPDP, which contains the functional groups pyridylthiol & NHS ester. This crosslinker can be used for enriching nitrosylated and glutathionylated proteins in a similar fashion as oxalyldihydrazide was described to do in this study.

### Conclusions

In this work, we present a proof of principle microfluidic enrichment of carbonylated proteins using oxalyldihydrazide as an immobilized crosslinker. Advantages of using this system to the conventional technique of affinity column chromatography include reduced sample consumption, reduced time, and minimized sample preparation steps. Because the process is done on a microfluidic platform, experiments can easily be run in parallel in order to achieve high-throughput protein analysis. When proteins are eluted from this system they are readily available for additional analysis, such as mass spectroscopy or electrophoresis. Because samples do not require derivatization prior to loading into the microchip, no additional considerations, such as molecular weight shift, need to be taken when the samples are analyzed further. In addition, because of the ease of modifying the surface of PMMA, the technique can be modified for analyzing other protein modifications present in diseased state tissue. This device can provide a stepping stone in the development of novel diagnostic technologies making use of biomarkers. The device also has immediate application for biomarker discovery research by taking advantage of its preconcentration ability.

### Acknowledgements

The project described was supported by Grant Number P20RR016456 from the National Center for Research Resources. The authors thank Mateusz Hupert for his expertise in micromilling techniques, Gergana Nestorova and Joe Nealy

for their assistance with the AFM usage, and Dongmei Cao for her assistance with the XPS studies. We thank Kinsey Cotton for her assistance with the images.

## References

- 1 R. L. Levine, J. A. Williams, E. R. Stadtman and E. Shacter, *Methods Enzymol.*, 1994, **233**, 346–357.
- 2 H. Mirzaei and F. Regnier, *Anal. Chem.*, 2005, **77**, 2386–2392.
- 3 R. J. Keller, N. C. Halmes, J. A. Hinson and N. R. Pumford, *Chem. Res. Toxicol.*, 1993, **993**, 430–433.
- 4 J. Bautista and M. D. Mateos-Nevado, *Biosci., Biotechnol., Biochem.*, 1998, **62**, 419–423.
- 5 J. Feng, H. Xie, D. L. Meany, L. V. Thompson, E. A. Arriaga and T. J. Griffin, *J. Gerontol., Ser. A*, 2008, **63**, 1137–1152.
- 6 Y. J. Suzuki, M. Carimi and D. A. Butterfield, *Antioxid. Redox Signaling*, 2010, **12**, 323–325.
- 7 E. R. Stadtman, *Ann. N. Y. Acad. Sci.*, 2001, **928**, 22–38.
- 8 A. G. Madian and F. E. Regnier, *J. Proteome Res.*, 2010, **2010**, 3366–3380.
- 9 Q. Wang, X. Zhao, S. He, Y. Liu, M. An and J. Ji, *Neurochem. Res.*, 2010, **35**, 13–21.
- 10 L. J. Yan and M. J. Forster, *J. Chromatogr., B: Anal. Technol. Biomed. Life Sci.*, **879**, 1308–1315.
- 11 J. Li, T. LeRiche, T. L. Tremblay, C. Wang, E. Bonneil, D. J. Harrison and P. Thibault, *Mol. Cell. Proteomics*, 2002, **1**, 157–168.
- 12 A. H. Diercks, A. Ozinsky, C. L. Hansen, J. M. Spotts, D. J. Rodriguez and A. Aderem, *Anal. Biochem.*, 2009, **386**, 30–35.
- 13 C. E. Robinson, A. Keshavarzian, D. S. Pasco, T. O. Frommel, D. H. Winship and E. W. Holmes, *Anal. Biochem.*, 1999, **266**, 48–57.
- 14 E. Barreiro, J. Gea, M. Di Falco, L. Kriazhev, S. James and S. N. Hussain, *Am. J. Respir. Cell Mol. Biol.*, 2005, **32**, 9–17.
- 15 R. L. Levine, D. Garland, C. N. Oliver, A. Amici, I. Climent, A. G. Lenz, B. W. Ahn, S. Shaltiel and E. R. Stadtman, *Methods Enzymol.*, 1990, **186**, 464–478.
- 16 B. W. Newton, W. K. Russell, D. H. Russell, S. K. Ramaiah and A. Jayaraman, *J. Proteome Res.*, 2009, **8**, 1663–1671.
- 17 N. Abello, B. Barroso, H. A. Kerstjens, D. S. Postma and R. Bischoff, *Talanta*, **80**, 1503–1512.
- 18 P. R. Jalili and H. L. Ball, *J. Am. Soc. Mass Spectrom.*, 2008, **19**, 741–750.
- 19 D. L. Meany, H. Xie, L. V. Thompson, E. A. Arriaga and T. J. Griffin, *Proteomics*, 2007, **7**, 1150–1163.
- 20 K. England and T. Cotter, *Biochem. Biophys. Res. Commun.*, 2004, **320**, 123–130.
- 21 B. K. Kristensen, P. Askerlund, N. V. Bykova, H. Egsgaard and I. M. Moller, *Phytochemistry*, 2004, **65**, 1839–1851.
- 22 H. Becker and L. E. Locascio, *Talanta*, 2002, **56**, 267–287.
- 23 T. B. Stachowiak, T. Rohr, E. F. Hilder, D. S. Peterson, M. Yi, F. Svec and J. M. Frechet, *Electrophoresis*, 2003, **24**, 3689–3693.
- 24 A. Amici, R. L. Levine, L. Tsai and E. R. Stadtman, *J. Biol. Chem.*, 1989, **264**, 3341–3346.
- 25 D. Pinto, E. A. Arriaga, R. M. Schoenherr, S. S. Chou and N. J. Dovichi, *J. Chromatogr., B: Anal. Technol. Biomed. Life Sci.*, 2003, **793**, 107–114.
- 26 M. L. Hupert, J. W. Guy, S. D. Llopis, H. Shadpour, S. Rani and N. D. E. and S. A. Soper, *Microfluid. Nanofluid.*, 2007, **3**, 1–11.
- 27 S. Wei, B. Vaidya, A. B. Patel, S. A. Soper and R. L. McCarley, *J. Phys. Chem. B*, 2005, **109**, 16988–16996.
- 28 M. R. Roe, H. Xie, S. Bandhakavi and T. J. Griffin, *Anal. Chem.*, 2007, **79**, 3747–3756.
- 29 P. DePhillips, I. Lagerlund, J. Farenmark and A. M. Lenhoff, *Anal. Chem.*, 2004, **76**, 5816–5822.
- 30 M. A. Galan and E. M. Martin del Valle, *Ind. Eng. Chem. Res.*, 2002, **41**, 2296–2304.

Downloaded by RSC Internal on 27 June 2012  
Published on 14 March 2012 on http://pubs.rsc.org | doi:10.1039/C2LC40103G